Electron Transfer in the Supramolecular Donor−Acceptor Dyad of Zinc Porphycene

Mamoru Fujitsuka,[†] Hisashi Shimakoshi,[‡] Sachiko Tojo,[†] Lingli Cheng,[†] Daisuke Maeda,[‡] Yoshio Hisaeda,[‡] and Tetsuro Majima*,[†]

Institute of Scientific and Industrial Research (SANKEN), Osaka University, Mihogaoka 8-1, Ibaraki, Osaka 567-0047, Japan, and Department of Chemistry and Biochemistry, Graduate School of Engineering, Kyushu University, Fukuoka 819-0395, Japan

Received: December 3, 2008; Revised Manuscript Received: January 26, 2009

The electron transfer processes of Zn octaethylporphycene (ZnPcn), a structural isomer of Zn octaethylporphyrin, have been investigated mainly using transient absorption spectroscopy. To form a supramolecular donor−acceptor dyad, imide compounds bearing a pyridine group at the N position of the imides have been used as an acceptor. The N atom of the pyridine ring can coordinate to the central Zn ion of ZnPcn. Formation of a supramolecular donor−acceptor dyad, that is, pentacoordinated ZnPcn, was confirmed by steady-state absorption spectroscopy using toluene as a solvent. Charge separation upon excitation of ZnPcn was indicated by efficient fluorescence quenching, especially when pyromellitic diimide was used as the acceptor. Electron transfer processes were confirmed by subpicosecond transient absorption spectroscopy, in which generation of a radical anion of the acceptor and a radical cation of ZnPcn, which was identified by means of γ-ray radiolysis, was confirmed. It became clear that the charge separation rate was smaller than that of the corresponding supramolecular dyads of Zn tetraphenylporphyrin and Zn octaethylporphyrin despite a similar driving force. This observation indicates a larger internal reorganization energy and a smaller coupling element of the ZnPcn dyad.

Introduction

Porphyrins have been investigated by many researchers because of their excellent properties applicable to many fields. For porphyrins, a series of isomers have been reported, porphycene, corrphycene, and hemiporphycene.[1] Characteristics of these isomers depending on their structures have become clearer recently. Porphycene was first synthesized by Vogel and co-workers in 1986.[2] Because of the lower symmetry of porphycene as compared to that of porphyrin, porphycene exhibits a large visible absorption, which is useful for application to photocatalysts, photodynamic therapy, and so on. Some of the present authors and their co-workers have also studied novel porphycene derivatives, which can be applicable to photodynamic therapy, etc.[3]

To date, reports on the electron transfer (ET) processes of porphycene derivatives are limited, as compared to many examples of ET studies on porphyrin derivatives. Levanon and his co-workers investigated the ET from a triplet excited free base and Zn-coordinated octaethylporphycenes to duroquinone, and they observed a radical anion of duroquinone by EPR.[4] Rubio et al. reported photoinduced intermolecular ET of H_2- and Pd-tetraphenylporphycenes.[5] Guldi et al. reported a one-electron oxidation and reduction of porphycenes by means of pulse radiolysis and γ-ray radiolysis.[6] D'Souza et al. reported the formation of a noncovalent donor−acceptor dyad of Zn porphycene and C_{60} derivatives.[7] They observed the fluorescence quenching of Zn porphycene in the dyad form, although the charge-separated state has not been confirmed by a spectroscopic method. For the detailed understanding of the ET processes, direct observation and characterization of the charge-separated state are indispensable.

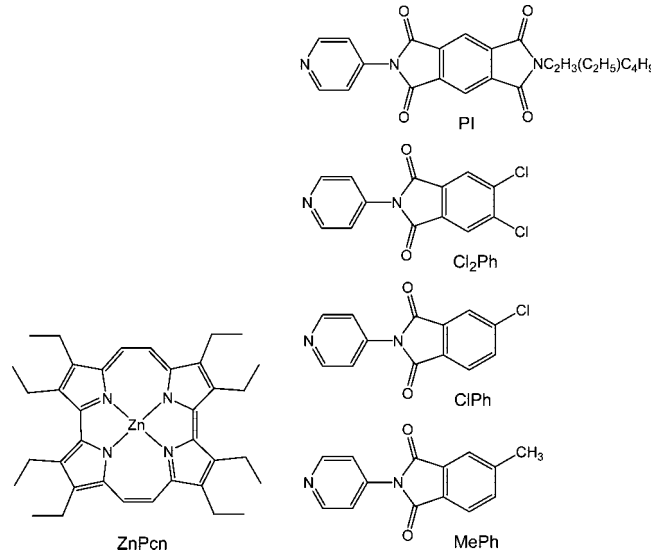

Figure 1. Molecular structures of ZnPcn and acceptors.

In the present study, we have investigated the ET processes of supramolecular donor−acceptor dyad molecules including Zn octaethylporphycene as a donor. The acceptor, the structure of which is indicated in Figure 1, was attached to the central Zn ion by means of coordination of a pyridine ring. Charge separation (CS) and recombination (CR) processes were successfully confirmed by observing transient absorption bands of the radical cation of porphycene and the radical anion of the acceptor during the subpicosecond laser flash photolysis.

* Corresponding author. E-mail: majima@sanken.osaka-u.ac.jp.
[†] Osaka University.
[‡] Kyushu University.

10.1021/jp810617a CCC: $40.75
Published on Web 03/12/2009

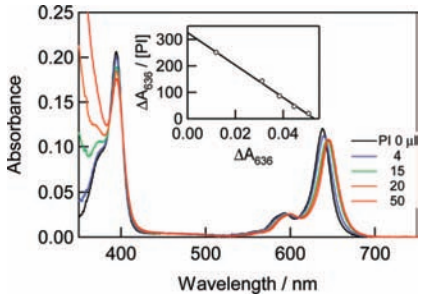

Figure 2. Absorption spectra observed during the complexation of PI and ZnPcn in toluene at room temperature. 4, 15, 20, and 50 μL of PI solution (12 mM) was added stepwise to ZnPcn (3.1 μM). Optical path is 5 mm. The inset shows the Scatchard plot of absorbance at 636 nm.

Characteristics of the ET processes of porphycene were revealed from a comparison with the ET processes of other porphyrin derivatives.

Experimental Section

Materials. 2,3,6,7,12,13,16,17-Octaethylporphycene (ZnPcn) was synthesized according to the reported procedure.[8] The synthesis of pyromellitic diimide bearing a pyridine ring at the N-position (Figure 1, PI) was reported in a previous paper.[9] Other phthalimides bearing a pyridine ring at the N-position (Figure 1, Cl_2Ph, ClPh, and CH_3Ph) were synthesized in a manner similar to that of PI using the corresponding phthalic anhydride as the starting material.

Apparatus. The subpicosecond transient absorption spectra were measured by the pump and probe method using a regeneratively amplified titanium sapphire laser as reported previously.[10] In the present study, the sample was excited using a 650 nm laser pulse, which was generated by an optical parametric amplifier. In the transient absorption measurements, complexes were prepared using an excess of the ligand. Judging from the association constant (vide infra), >96% of ZnPcn was in the complex form.

The fluorescence decay profiles were measured by the single photon counting method using a streakscope.[11] The ultrashort laser pulse was generated by a Ti:sapphire laser. For excitation of the sample, the output of the Ti:sapphire laser was converted to the second harmonic oscillation (400 nm) using a BBO type I crystal.

γ-Ray radiolysis of the sample was carried out using ^{60}Co source of ISIR, Osaka University. After the freeze pump thaw cycles, the sample was cooled at 77 K to form a transparent glass, which was then irradiated with γ-ray. In the present study, *n*-butylchloride was used as a solvent to form the radical cation of the substrate.[12]

The steady-state absorption and fluorescence spectra were measured using a Shimadzu UV-3100PC and Hitachi 850, respectively. Optimized structures were estimated at the B3LYP/6-31G* level using the Gaussian 03 package.[13]

Results and Discussion

Absorption and Fluorescence Spectra. Figure 2 shows the absorption spectra of ZnPcn and its complex with PI in toluene. ZnPcn shows characteristic absorption bands at 636 and 594 nm due to the Q-band and 394 nm due to the Soret band. Upon excitation, ZnPcn shows fluorescence with a peak at 649 nm. The quantum yield has been reported to be 0.05 by Levanon and his co-workers.[4] The fluorescence lifetime was measured by the single photon counting method to be 3.9 ns.

When PI in toluene was added stepwise to the solution of ZnPcn, the absorption peaks showed obvious changes as shown in Figure 2. The Soret band decreased in intensity and the Q-band shifted to a longer wavelength side (646 and 601 nm), showing isosbestic points at 643, 609, and 598 nm. These spectral changes can be attributed to the formation of pentacoordinated ZnPcn by means of coordination of the N-atom of pyridine to the central Zn ion.[7] A similar spectral change has been observed with the coordination of pyridine (Py) and phthalimides to ZnPcn (Table 1). Association constants (K_a) were estimated by means of a Scatchard plot to be 5300−30 000 M^{-1} (Table 1).[14] The estimated values are similar to those reported by previous researchers.[7] In the fluorescence and transient absorption studies, excess amounts of PI or phthalimides were added to ZnPcn to ensure that ≥96% of ZnPcn is in the pentacoordinated form.

When Py is coordinated to ZnPcn, a fluorescence peak was observed at 662 nm, which is red-shifted by 13 nm as compared to that of pristine ZnPcn in toluene. The fluorescence intensity decreased by a factor of 0.62. The fluorescence lifetime was 3.3 ns. When phthalimides (Cl_2Ph, ClPh, and CH_3Ph) were added to ZnPcn, similar changes in fluorescence properties, that is, a red-shifted fluorescence peak, reduced intensity, and a shortened fluorescence lifetime, were observed. Cl_2Ph−ZnPcn showed a slightly shortened lifetime as compared to ZnPcn coordinated by ClPh, CH_3Ph, or Py. On the other hand, when PI was added to ZnPcn, the fluorescence intensity showed a dramatic decrease by a factor of 0.05. The fluorescence decayed by two components, that is, 0.14 (94%) and 3.9 ns (6%), of which the latter can be attributed to ZnPcn not in the complex form, because the lifetime is the same as that of the pristine ZnPcn. Because the acceptor ability of PI is higher than that of other ligands investigated, CS in the singlet excited state of ZnPcn is indicated.

Molecular Orbital Calculation. Structures of the complex were estimated by means of molecular orbital calculation. Figure 3 shows the optimized molecular structure of PI−ZnPcn and the pattern of the HOMO, LUMO, and LUMO+2. In the calculation, the alkyl groups of PI−ZnPcn were reduced to a methyl group for simplicity. The N atom of the pyridine ring

TABLE 1: Absorption, Fluorescence, and Association Constant of ZnPcn and Its Complexes in Toluene[a]

	λ_{abs}/nm	λ_f/nm	Φ_f	τ_f/ns	K_a/M^{-1}
ZnPcn	394, 594, 636	649	0.05[b]	3.9 (100%)	
Py−ZnPcn	396, 602, 647	662	0.03	3.3 (100%)	30 000
PI−ZnPcn	394, 601, 646	660	0.003	0.14 (94%), 3.9 (6%)	6100
Cl_2Ph−ZnPcn	394, 601, 646	661	0.03	3.1 (100%)	5300
ClPh−ZnPcn	395, 602, 647	662	0.03	3.3 (100%)	8100
MePh−ZnPcn	396, 601, 647	661	0.02	3.3 (100%)	11 000

[a] λ_{abs}, λ_f, Φ_f, and τ_f indicate absorption and fluorescence peaks, fluorescence quantum yield, and fluorescence lifetime, respectively. [b] From ref 4.

TABLE 2: Oxidation and Reduction Potentials of Complexes and Driving Force for Electron Transfers

	E_{ox}/V vs SCE	E_{red}/V vs SCE[b]	$-\Delta G_{CS}$/eV[c]	$-\Delta G_{CR}$/eV[c]
Py−ZnPcn	0.47[a]			
PI−ZnPcn		−0.83	0.69	1.19
Cl_2Ph−ZnPcn		−1.44	0.10	1.78
ClPh−ZnPcn		−1.56	−0.02	1.90
MePh−ZnPcn		−1.70	−0.16	2.04

[a] Data from ref 7. [b] The reduction potentials were estimated by cyclic voltammetry in 50 mM $TEAClO_4$ dichloromethane. The scan rate was 100 mV s^{-1}. [c] The listed values were calculated using 5.0 Å as r_D. r_A values for PI and phthalimides were 3.5 and 3.0 Å, respectively. r values for PI−ZnPcn and phthalimide−ZnPcn were 9.8 and 8.6 Å, respectively. ΔG_S was decreased by 0.35 eV according to ref 16.

of PI forms a bond with the central Zn ion of ZnPcn. The bond length was estimated to be 2.17 Å. By formation of pentacoordinated ZnPcn, the Zn ion is slightly pulled out from the Pcn plane by 0.44 Å, which is a value similar to those estimated for other PI-coordinated tetrapyrrole macrocycles.[9] The center-to-center distance of PI−ZnPcn was estimated to be 9.8 Å. For other phthalimide−ZnPcn complexes, the center-to-center distance was 8.6 Å.

For PI−ZnPcn, the HOMO is localized on ZnPcn. The LUMO of ZnPcn corresponds to the LUMO+2 of PI−ZnPcn. On the other hand, the LUMO of PI−ZnPcn is on PI. Thus, a photoinduced CS is expected when ZnPcn of the complex is excited. In the CS process, the pyridine ring will act as a spacer, because the LUMO is localized on pyromellitic diimide and not on the pyridine ring.

Driving Force for Electron Transfer. To estimate the driving force ($-\Delta G$) for ET, the reduction potentials of phthalimides were measured by cyclic voltammetry. The estimated values are summarized in Table 2. The reduction potential of PI was estimated in a previous paper.[9] The oxidation potential of coordinated ZnPcn was reported by D'Souza et al.[7] By using the oxidation and reduction potentials and other geometrical parameters estimated by molecular orbital calculation, the driving force for the ET (ΔG_{CS} and ΔG_{CR}) was estimated using the following equations:[15]

$$-\Delta G_{CS} = \Delta E_{0-0} - (-\Delta G_{CR}) \quad (1)$$

$$-\Delta G_{CR} = E_{ox} - E_{red} + \Delta G_S \quad (2)$$

$$\Delta G_S = e^2/(4\pi\varepsilon_0)[(1/(2r_D) + 1/(2r_A) - 1/r)(1/\varepsilon_s) - (1/(2r_D) + 1/(2r_A))(1/\varepsilon_r)] \quad (3)$$

where ΔE_{0-0} is the excitation energy, r_D and r_A are the ionic radii of the donor and acceptor, respectively, r is the center-to-center distance, and ε_s are ε_r are dielectric constants of the solvent for the rate measurements and redox measurements, respectively. The ΔG_S value was reduced by 0.35 eV according to ref 16. The estimated ΔG values are summarized in Table 2. For PI−ZnPcn and Cl_2Ph−ZnPcn, the ΔG_{CS} values are negative, indicating that CS is the possible process. On the other hand, for ClPh−ZnPcn and CH_3Ph−ZnPcn, positive ΔG_{CS} values indicate that CS is not preferable in these dyads. Actually, the fluorescence lifetimes of ClPh−ZnPcn and CH_3Ph−ZnPcn are the same as that of Py−ZnPcn, indicating the absence of a CS process. The substantially shortened fluorescence lifetime of PI−ZnPcn is in accordance with the larger $-\Delta G_{CS}$ value. The slightly shortened lifetime of Cl_2Ph−ZnPcn indicates an inefficient CS due to the small $-\Delta G_{CS}$ value. For complete understanding of the ET process, a transient absorption study is indispensable.

Absorption Spectrum of Radical Cation of ZnPcn. For investigation of the ET processes by transient absorption spectroscopy, observation of a donor radical cation and an acceptor radical anion is essential. For PI, the radical anion of pyromellitic diimide is reported to show a sharp peak around 720 nm.[9,17,18] On the other hand, the absorption spectrum of the radical cation of ZnPcn has not been reported. In the present study, we irradiated γ-ray to ZnPcn in *n*-butylchloride solution at 77 K. It is established that the γ-ray irradiation of the substrate in *n*-butylchloride at 77 K generates the radical cation of the substrate efficiently.[12] Figure 4 shows an absorption spectrum of ZnPcn in *n*-butylchloride after γ-ray irradiation. A clear absorption peak appeared at 860 nm, which can be attributed to the radical cation of ZnPcn. Guldi and his co-workers reported the absorption spectra of radical cations of H_2-, Cu(II)-, Fe(III)-,

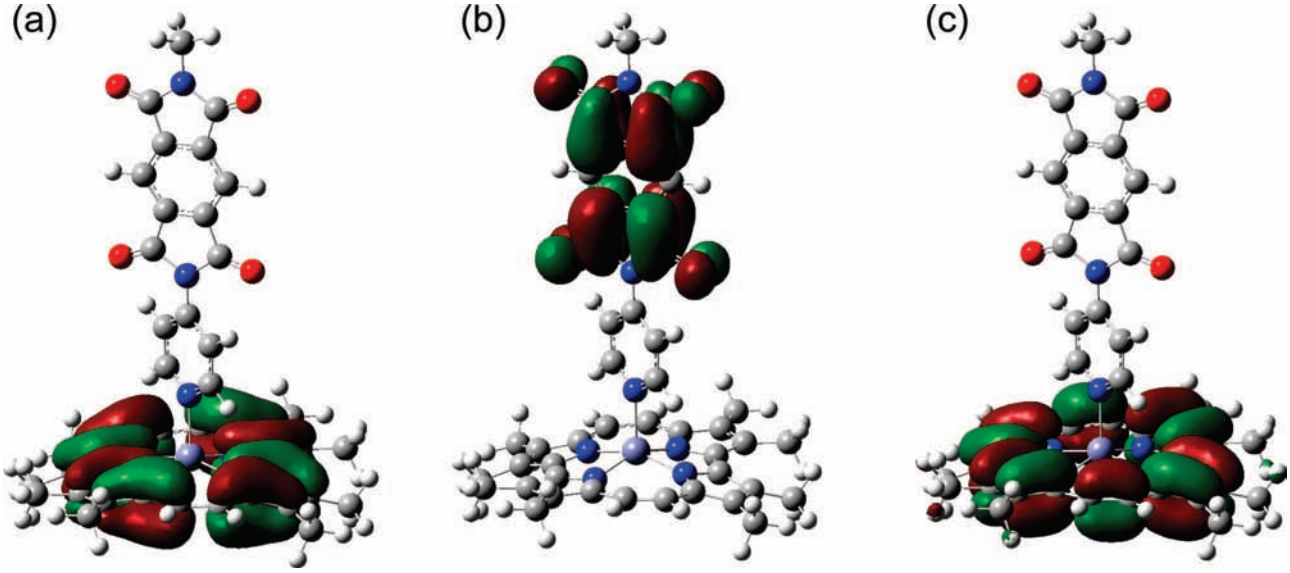

Figure 3. Structure of the complex of PI and ZnPcn calculated at the B3LYP/6-31G* level with the Gaussian 03 package. HOMO (a), LUMO (b), and LUMO+2 (c) were indicated. Alkyl groups of ZnPcn and PI were reduced to methyl group.

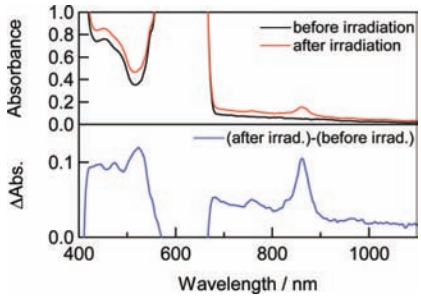

Figure 4. (Upper panel) Absorption spectra of ZnPcn in *n*-butylchloride at 77 K before (black) and after γ-ray irradiation (red). (Lower panel) Difference spectrum.

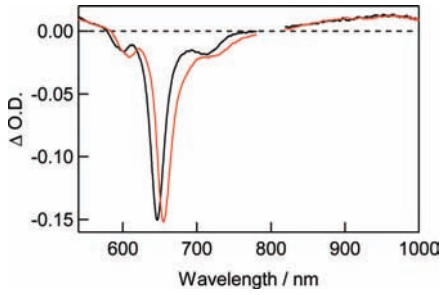

Figure 5. Transient absorption spectra of ZnPcn (black) and Py−ZnPcn (red) in toluene at 10 ps after the excitation by 650 nm femtosecond laser pulse.

Co(II)-, and Ni(II)-coordinated tetrapropylporphycenes, although their spectral range is limited to 840 nm in the near-IR region.[6b] They reported that the radical cation of Co(III)- and Ni(III)-coordinated tetrapropylporphycenes showed an absorption band around 820 nm due to a π-radical cation. Thus, the present result resembles theirs.

Electron Transfer in ZnPcn Complexes. At first, the absorption spectra of singlet-excited ZnPcn and pentacoordinated ZnPcn were measured by means of laser flash spectroscopy as references. Because both ZnPcn and pentacoordinated ZnPcn have strong absorption around 650 nm, the photoinduced processes of these compounds were examined using a 650 nm femtosecond laser pulse as an excitation source. Figure 5 shows the absorption spectra of ZnPcn and Py−ZnPcn at 10 ps after the 650 nm laser excitation during the laser flash photolysis. Both show bleaching due to the Q-band absorption and S_1-S_n absorption at 960 nm as well as a stimulated emission band at the red edge of the bleaching due to the Q-band. These spectral features continued for a few nanoseconds in accordance with their 3−4 ns of singlet excited-state lifetime.

Transient absorption spectra of PI−ZnPcn excited by a 650 nm laser are shown in Figure 6. The spectrum at 10 ps after the excitation is the same as that of Py−ZnPcn. With time, the absorption band at 960 nm decreased and new absorption bands appeared at 890 and 720 nm, which can be attributed to the radical cation of ZnPcn and the radical anion of PI, respectively. A slight change in the peak position of the radical cation may result from the pentacoordination of ZnPcn and the differences in temperature and solvent. These results indicate the formation of a CS state from the singlet excited ZnPcn. The lower panel of Figure 6 shows the kinetic trace of ΔO.D. at 720 nm during the laser flash photolysis. Immediately after the laser excitation, the ΔO.D. at 720 nm is negative because of stimulated emission from ZnPcn. With delay time, the kinetic trace shows a rise due to CS and reached a maximum around 300 ps after the excitation. The kinetic trace then shows a gradual decay due to CR. Because the additional absorption was not observed at a

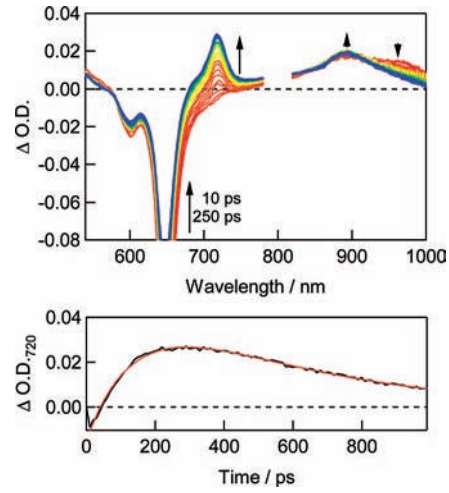

Figure 6. Transient absorption spectra of PI−ZnPcn in toluene during the laser flash photolysis using 650 nm femtosecond pulse for excitation. Spectra were obtained from 10 to 250 ps (10 ps step) after the laser excitation. Lower panel is kinetic trace of ΔO.D. at 720 nm during the laser flash photolysis. The red curve is the fitted curve.

few nanoseconds after the excitation, it is indicated that CR generates the ground state of PI−ZnPcn. The kinetic trace was analyzed taking the decay of stimulated emission, CS, and CR into account. The time constant for the rise component was estimated to be 7.0×10^9 s^{-1}, which is in good accordance with the fluorescence lifetime of PI−ZnPcn ($1/\tau_f = 7.1 \times 10^9$ s^{-1}), supporting the belief that the rise profile indicates the CS process. Because the CS process competes with the deactivation process of ZnPcn, the CS rate (k_{CS}) can be estimated using the relation, $k_{CS} = \tau_f(\text{PI}-\text{ZnPcn})^{-1} - \tau_f(\text{Py}-\text{ZnPcn})^{-1}$, where τ_f(PI−ZnPcn) and τ_f(Py−ZnPcn) are fluorescence lifetimes of PI−ZnPcn and Py−ZnPcn, respectively, being 6.8×10^9 s^{-1}. The yield of the CS was calculated to be 0.96, indicating an efficient CS process. The decay time constant of the kinetic trace of ΔO.D., that is, CR rate (k_{CR}), was estimated to be 2.4×10^9 s^{-1}, which corresponds to 430 ps of the CS state lifetime.

As indicated above, the fluorescence lifetime of Cl_2Ph−ZnPcn is slightly shorter than that of Py−ZnPcn. From the driving force, the CS in Cl_2Ph−ZnPcn is expected, although the efficiency is expected to be low because of a small $-\Delta G_{CS}$ value. From the transient absorption spectra, the generation of the CS state was difficult to see. Assuming that the shortening of the fluorescence lifetime is due to CS, the rate constant and quantum yield of CS were estimated to be 2×10^7 s^{-1} and 0.06, respectively.

In the previous study, we have investigated ET processes in complexes of PI and four tetrapyrrole macrocycles, that is, Zn tetraphenylporphyrin (ZnTPP), Zn octaethylporphyrin (ZnOEP), Zn phthalocyanine, and Zn naphthalocyanine.[9] Among them, the $-\Delta G_{CS}$ values of PI−ZnTPP (0.62 eV) and PI−ZnOEP (0.83 eV) are close to that of PI−ZnPcn (0.69 eV). The respective CS rates of PI−ZnTPP and PI−ZnOEP were 5.6×10^{10} and 1.1×10^{11} s^{-1}, which are larger than that of PI−ZnPcn (6.8×10^9 s^{-1}) despite similar $-\Delta G_{CS}$ values. On the other hand, the CR rates are similar, 1.4×10^9, 2.7×10^9, and 2.8×10^9 s^{-1} for PI−ZnTPP, PI−ZnOEP, and PI−ZnPcn, respectively. Therefore, ZnPcn showed ET behavior different from that of other tetrapyrrole macrocycles.

To explain the observed difference in the CS rate, the observed ET processes are discussed on the basis of the Marcus theory.[19] In Figure 7, the estimated ET rates (k_{CS} and k_{CR}) are

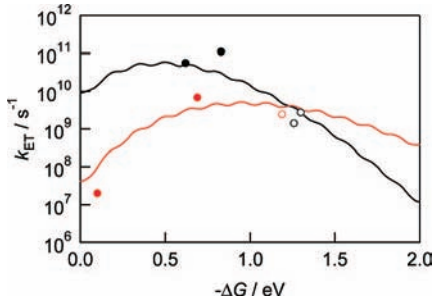

Figure 7. Free energy change ($-\Delta G$) dependence of ET rate (k_{ET}, i.e., k_{CS} (●) and k_{CR} (○)) of porphyrins (black) and porphycene (red) complexes. Black curve was calculated using eq 4 in the text by assuming $\lambda_s = 0.05$ eV, $V = 0.002$ eV, $\hbar\langle\omega\rangle = 0.15$ eV, and $\lambda_v = 0.5$ eV for porphyrins. Red curve was calculated by changing V and λ_v to 0.0007 and 1.0 eV, respectively.

plotted against the free energy changes. Usually, the ET rate depends on the free energy change according to eqs 4−6:

$$k_{ET} = \sqrt{\frac{\pi}{\hbar^2 \lambda_S k_B T}} |V|^2 \sum_m (e^{-S}(S^m/m!)) \exp\left(-\frac{(\lambda_S + \Delta G + m\hbar\langle\omega\rangle)^2}{4\lambda_S k_B T}\right) \quad (4)$$

$$\lambda_S = e^2\left(\frac{1}{2r_D} + \frac{1}{2r_A} - \frac{1}{r}\right)\left(\frac{1}{n^2} - \frac{1}{\varepsilon_S}\right) \quad (5)$$

$$S = \frac{\lambda_V}{\hbar\langle\omega\rangle} \quad (6)$$

In eq 4, λ_S is the solvent reorganization energy given by eq 5, V is the electronic coupling, S is the electron−vibration coupling constant given by eq 6, and $\langle\omega\rangle$ is the averaged angular frequency. In eq 5, n is the refractive index. In eq 6, λ_V is the internal reorganization energy. Using the values listed in the footnote of Table 2, the λ_S value was estimated to be 0.05 eV. In Figure 7, eq 4 was calculated as a black curve by assuming λ_V, V, and $\hbar\langle\omega\rangle$ to be 0.5, 0.002, and 0.15 eV, respectively. Here, 0.5 eV of λ_V was employed, because the λ_V values for ET from the various S_1-excited Zn porphyrin derivatives have been reported to be 0.3−0.6 V.[20] The calculated curve well reproduced the k_{CS} and k_{CR} values of PI−ZnTPP and PI−ZnOEP. It is clear that the CS rate of PI−ZnPcn is not on the black curve. Thus, for the ET process of ZnPcn, a different Marcus parabola has to be considered. Because the λ_S and $\hbar\langle\omega\rangle$ values of ZnPcn are assumed to be not so different from those of porphyrins, the λ_V and V values were changed. The red curve, which is close to the experimental data, was obtained by employing 1.0 and 0.0007 eV of λ_V and V values, respectively. Because the data points for this analysis are limited at the present stage of our experiments, the validity of the estimated parameters is not clear. However, the tendency for ZnPcn to assume large λ_V and small V values will be characteristic of the ET systems of porphycenes.

Conclusions

In the present study, we investigated the photoinduced ET processes of a supramolecular donor−acceptor dyad of ZnPcn and an acceptor ligand. Although formation of the supramolecular dyad was confirmed for all ligands investigated, a CS process was confirmed for PI−ZnPcn, which shows a substantial decrease in the fluorescence intensity of ZnPcn. The CS and CR processes in PI−ZnPcn were clearly confirmed by subpicosecond laser flash spectroscopy, which revealed the formation of a ZnPcn radical cation and a radical anion of the acceptor. It became clear that the CS and CR rates were not explained using the Marcus parabola estimated for porphyrin derivatives. Larger λ_V and smaller V values as compared to those of porphyrins have to be employed to explain the behavior of the ZnPcn.

Acknowledgment. We thank the members of the Radiation Laboratory of ISIR, Osaka University. This work has been partly supported by a Grant-in-Aid for Scientific Research (Project 17105005, 19350069, Priority Area (477), and others) from the Ministry of Education, Culture, Sports, Science, and Technology (MEXT) of the Japanese Government.

References and Notes

(1) Fowler, C. J.; Sessler, J. L.; Lynch, V. M.; Waluk, J.; Gebauer, A.; Lex, J.; Heger, A.; Zuniga-y-Rivero, F.; Vogel, E. *Chem.-Eur. J.* **2002**, *8*, 3485.

(2) Vogel, E.; Köcher, M.; Schmickler, H.; Lex, J. *Angew. Chem., Int. Ed. Engl.* **1986**, *25*, 257.

(3) (a) Hayashi, T.; Dejima, H.; Matsuo, T.; Sato, H.; Murata, D.; Hisaeda, Y. *J. Am. Chem. Soc.* **2002**, *124*, 11226. (b) Hayashi, T.; Nakashima, Y.; Ito, K.; Ikegami, T.; Aritome, I.; Aoyagi, K.; Ando, T.; Hisaeda, Y. *Inorg. Chem.* **2003**, *42*, 7345. (c) Hayashi, T.; Nakashima, Y.; Ito, K.; Ikegami, T.; Aritome, I.; Hisaeda, Y. *Org. Lett.* **2003**, *5*, 2845. (d) Matsuo, T.; Murata, D.; Hisaeda, Y.; Hori, H.; Hayashi, T. *J. Am. Chem. Soc.* **2007**, *129*, 12906. (e) Ito, K.; Matsuo, T.; Aritome, I.; Hisaeda, Y.; Hayashi, T. *Bull. Chem. Soc. Jpn.* **2008**, *81*, 76. (f) Shimakoshi, H.; Baba, T.; Iseki, Y.; Aritome, I.; Endo, A.; Adachi, C.; Hisaeda, Y. *Chem. Commun.* **2008**, 2882. (g) Shimakosi, H.; Baba, T.; Iseki, Y.; Endo, A.; Adachi, C.; Watanabe, M.; Hisaeda, Y. *Tetrtahedron Lett.* **2008**, *49*, 6198. (h) Baba, T.; Shimakoshi, H.; Endo, A.; Adachi, C.; Hisaeda, Y. *Chem. Lett.* **2008**, *37*, 264. (i) Maeda, D.; Shimakosi, H.; Abe, M.; Hisaeda, Y. *Dalton Trans.* **2009**, 140.

(4) Berman, A.; Mchaeli, A.; Feitelson, J.; Bowman, M. K.; Norris, J. R.; Levanon, H.; Vogel, E.; Koch, P. *J. Phys. Chem.* **1992**, *96*, 3041.

(5) Rubi, N.; Borrell, J. I.; Teixidó, J.; Cañete, M.; Juarranz, Á.; Villanueva, Á.; Stockert, J. C.; Nonell, S. *Photochem. Photobiol. Sci.* **2006**, *5*, 376.

(6) (a) Guldi, D. M.; Neta, P.; Vogel, E. *J. Phys. Chem.* **1996**, *100*, 4097. (b) Guldi, D. M.; Field, J.; Grodkowski, J.; Neta, P.; Vogel, E. *J. Phys. Chem.* **1996**, *100*, 13609.

(7) D'Souza, F.; Deviprasad, G. R.; Rahman, M. S.; Choi, J.-P. *Inorg. Chem.* **1999**, *38*, 2157.

(8) Vogel, E.; Koch, P.; Hou, X.-L.; Lex, J.; Lausmann, M.; Kisters, M.; Aukauloo, M. A.; Richard, P.; Guilard, R. *Angew. Chem., Int. Ed. Engl.* **1993**, *32*, 1600.

(9) Harada, K.; Fujitsuka, M.; Sugimoto, A.; Majima, T. *J. Phys. Chem. A* **2007**, *111*, 11430.

(10) Fujitsuka, M.; Cho, D. W.; Tojo, S.; Inoue, A.; Shiragami, T.; Yasuda, M.; Majima, T. *J. Phys. Chem. A* **2007**, *111*, 10574.

(11) Fujitsuka, M.; Okada, A.; Tojo, S.; Takei, F.; Onitsuka, K.; Takahashi, S.; Majima, T. *J. Phys. Chem. B* **2004**, *108*, 11935.

(12) Shida, T. *Electronic Absorption Spectra of Radical Ions*; Elsevier: Amsterdam, 1988.

(13) Frisch, M. J.; Trucks, G. W.; Schlegel, H. B.; Scuseria, G. E.; Robb, M. A.; Cheeseman, J. R.; Montgomery J.A., Jr.; Vreven, T.; Kudin, K. N.; Burant, J. C.; Millam, J. M.; Iyengar, S. S.; Tomasi, J.; Barone, V.; Mennucci, B.; Cossi, M.; Scalmani, G.; Rega, N.; Petersson, G. A.; Nakatsuji, H.; Hada, M.; Ehara, M.; Toyota, K.; Fukuda, R.; Hasegawa, J.; Ishida, M.; Nakajima, T.; Honda, Y.; Kitao, O.; Nakai, H.; Klene, M.; Li, X.; Knox, J. E.; Hratchian, H. P.; Cross, J. B.; Bakken, V.; Adamo, C.; Jaramillo, J.; Gomperts, R.; Stratmann, R. E.; Yazyev, O.; Austin, A. J.; Cammi, R.; Pomelli, C.; Ochterski, J. W.; Ayala, P. Y.; Morokuma, K.; Voth, G. A.; Salvador, P.; Dannenberg, J. J.; Zakrzewski, V. G.; Dapprich, S.; Daniels, A. D.; Strain, M. C.; Farkas, O.; Malick, D. K.; Rabuck, A. D.; Raghavachari, K.; Foresman, J. B.; Ortiz, J. V.; Cui, Q.; Baboul, A. G.; Clifford, S.; Cioslowski, J.; Stefanov, B. B.; Liu, G.; Liashenko, A.; Piskorz, P.; Komaromi, I.; Martin, R. L.; Fox, D. J.; Keith, T.; Al Laham, M. A.; Peng, C. Y.; Nanayakkara, A.; Challacombe, M.; Gill, P. M. W.; Johnson, B.; Chen, W.; Wong, M. W.; Gonzalez, C.; Pople, J. A. *Gaussian 03*; Gaussian, Inc.: Wallingford, CT, 2004.

(14) Scatchard, G. *Ann. N.Y. Acad. Sci.* **1949**, *51*, 660.

(15) Weller, A. *Z. Phys. Chem. Neue Folge* **1982**, *133*, 93.

(16) Mataga, N.; Chosrowjan, H.; Taniguchi, S.; Shibata, Y.; Yoshida, N.; Osuka, A.; Kikuzawa, T.; Okada, T. *J. Phys. Chem. A* **2002**, *106*, 12191.
(17) Osuka, A.; Nakajima, S.; Maruyama, K.; Mataga, N.; Asahi, T.; Yamazaki, I.; Nishimura, Y.; Ohono, T.; Nazaki, K. *J. Am. Chem. Soc.* **1993**, *115*, 4577.
(18) Wiederrech, G. P.; Niemczyk, M. P.; Svec, W. A.; Wasielewski, M. R. *J. Am. Chem. Soc.* **1996**, *118*, 81.
(19) (a) Marcus, R. A. *Annu. Rev. Phys. Chem.* **1964**, *15*, 144. (b) Marcus, R. A.; Sutin, N. *Biochim. Biophys. Acta* **1985**, *811*, 265. (c) Marcus, R. A. *Angew. Chem., Int. Ed. Engl.* **1993**, *32*, 1111.
(20) (a) Gaines, G. L., III; O'Neil, M. P.; Svec, W. A.; Niemczyk, M. P.; Wasielewski, M. R. *J. Am. Chem. Soc.* **1991**, *113*, 719. (b) Asahi, T.; Ohkohchi, M.; Matsusaka, R.; Mataga, N.; Zhang, R. P.; Osuka, A.; Maruyama, K. *J. Am. Chem. Soc.* **1993**, *115*, 5665. (c) Heitele, H.; Pöllinger, F.; Häberle, T.; Michel-Beyerle, M. E.; Staab, H. A. *J. Phys. Chem.* **1994**, *98*, 7402. (d) DeGraziano, J. M.; Liddell, P. A.; Legett, L.; Moore, A. L.; Moore, T. A.; Gust, D. *J. Phys. Chem.* **1994**, *98*, 1758. (e) Häberle, T.; Hirsh, J.; Pöllinger, F.; Heitele, H.; Michel-Beyerle, M. E.; Anders, C.; Döhling, A.; Krieger, C.; Rückemann, A.; Staab, H. A. *J. Phys. Chem.* **1996**, *100*, 18269. (f) Osuka, A.; Noya, G.; Taniguchi, S.; Okada, T.; Nishimura, Y.; Yamazaki, I.; Mataga, N. *Chem.-Eur. J.* **2000**, *6*, 33.

JP810617A